AGU PUBLICATIONS

Water Resources Research

RESEARCH ARTICLE
10.1002/2016WR018663

Key Points:
- Four-year catchment-scale water balances of a tree plantation and pasture were compared
- Frequency of rainfall events appeared to be crucial in driving annual streamflow
- Detailed topography and geology information is key to modeling ephemeral catchment hydrology

Supporting Information:
- Supporting Information S1

Correspondence to:
J. F. Dean,
j.f.dean@vu.nl

Citation:
Dean, J. F., M. Camporese, J. A. Webb, S. P. Grover, P. E. Dresel, and E. Daly (2016), Water balance complexities in ephemeral catchments with different land uses: Insights from monitoring and distributed hydrologic modeling, *Water Resour. Res.*, *52*, 4713–4729, doi:10.1002/2016WR018663.

Received 1 FEB 2016
Accepted 22 MAY 2016
Accepted article online 26 MAY 2016
Published online 19 JUN 2016

Water balance complexities in ephemeral catchments with different land uses: Insights from monitoring and distributed hydrologic modeling

J. F. Dean[1,2,3], M. Camporese[4], J. A. Webb[1,2], S. P. Grover[5], P. E. Dresel[6], and E. Daly[2,7]

[1]Department of Ecology, Environment and Evolution, La Trobe University, Melbourne, Victoria, Australia, [2]National Centre for Groundwater Research and Training, Flinders University, Adelaide, South Australia, Australia, [3]Now at Earth and Climate Cluster, Faculty of Earth and Life Sciences, Vrije Universiteit Amsterdam, Amsterdam, Netherlands, [4]Department of Civil, Environmental and Architectural Engineering, University of Padua, Padua, Italy, [5]Department of Animal, Plant and Soil Sciences, La Trobe University, Melbourne, Victoria, Australia, [6]Department of Economic Development, Jobs, Transport and Resources, Bendigo, Victoria, Australia, [7]Department of Civil Engineering, Monash University, Melbourne, Victoria, Australia

Abstract Although ephemeral catchments are widespread in arid and semiarid climates, the relationship of their water balance with climate, geology, topography, and land cover is poorly known. Here we use 4 years (2011–2014) of rainfall, streamflow, and groundwater level measurements to estimate the water balance components in two adjacent ephemeral catchments in south-eastern Australia, with one catchment planted with young eucalypts and the other dedicated to grazing pasture. To corroborate the interpretation of the observations, the physically based hydrological model CATHY was calibrated and validated against the data in the two catchments. The estimated water balances showed that despite a significant decline in groundwater level and greater evapotranspiration in the eucalypt catchment (104–119% of rainfall) compared with the pasture catchment (95–104% of rainfall), streamflow consistently accounted for 1–4% of rainfall in both catchments for the entire study period. Streamflow in the two catchments was mostly driven by the rainfall regime, particularly rainfall frequency (i.e., the number of rain days per year), while the downslope orientation of the plantation furrows also promoted runoff. With minimum calibration, the model was able to adequately reproduce the periods of flow in both catchments in all years. Although streamflow and groundwater levels were better reproduced in the pasture than in the plantation, model-computed water balance terms confirmed the estimates from the observations in both catchments. Overall, the interplay of climate, topography, and geology seems to overshadow the effect of land use in the study catchments, indicating that the management of ephemeral catchments remains highly challenging.

1. Introduction

Land use and land use change play key roles in the human-induced environmental change that the world is currently experiencing [*Sterling et al.*, 2012], increasing pressures on natural resources in managed landscapes [*Foley et al.*, 2005]. The growing demand for food requires intensive use of land for agricultural production and grazing, with consequent depletion of groundwater resources [*Famiglietti*, 2014]; at the same time, unused or degraded agricultural land is often converted to tree plantations for timber production or carbon bio-sequestration [*Jackson et al.*, 2005].

In rural catchments, it has been observed worldwide that the establishment of plantations tends to reduce streamflow at the catchment outlet, thereby reducing fresh water resources available for downstream users and ecosystems [*Brown et al.*, 2005]. This reduction is attributed to the larger interception and water use of trees when compared with pasture and crops. The deeper root system of trees reduces groundwater recharge and may lead to direct uptake of groundwater for transpiration [*Engel et al.*, 2005; *Benyon et al.*, 2006; *Feikema et al.*, 2010; *Nosetto et al.*, 2012]. Since water availability at catchment outlets is important for human uses and to sustain ecosystems [*Snyder and Williams*, 2000; *Smakhtin*, 2001], considerable effort has been devoted to understanding the links between land use and streamflow, largely through paired catchment experiments [e.g., *Brown et al.*, 2005]. Most of the available studies refer to perennial streams in

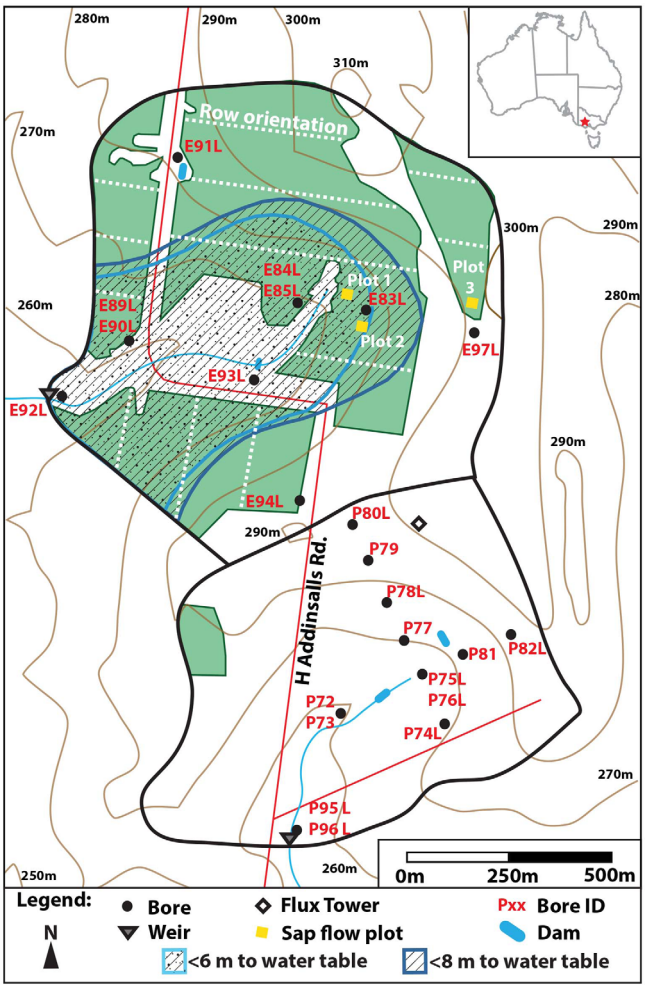

Figure 1. Eucalypt catchment and pasture catchment, and the location of the streams, weirs and bores and their reference numbers; "L" denotes the presence of a water level logger in the bores. Green is tree cover and white is pasture cover; tree row orientation is indicated by the dashed white lines. Average depth to water table relevant to tree rooting depths for *E. globulus* [*Benyon et al*., 2006] is shown for the Eucalypt catchment only (30% of catchment has root depth lower than 6 m, and 38% of catchment lower than 8 m). The inset shows the location of study site in Australia.

catchments with average annual precipitation greater than 800 mm [*Brown et al*., 2005; *Farley et al*., 2005; *Jackson et al*., 2005]. These studies focused on streamflow, with little data on groundwater levels. In lower rainfall regions and ephemeral catchments, where evapotranspiration might equal or exceed annual rainfall, the dearth of experimental observations makes estimates and predictions of the relationship between land use and water resources highly uncertain [*Jackson et al*., 2009; *Dye*, 2013]. The processes leading to runoff generation in ephemeral catchments have not been studied in depth and are strongly dependent on the combined effect of climate, catchment geology and topography as well as land use. At the regional scale, the effect of land use has been observed to have a lower effect than annual rainfall and catchment characteristics other than land cover [e.g., *Chiverton et al*., 2015]. In a southeastern Australian example, *Yhidego and Webb* [2011] found that climate, especially rainfall, was the main driver of groundwater levels, with land cover playing a secondary role based on statistical models that reproduced groundwater levels in three local aquifers. Likewise, *Brown et al*. [2015] found that at regional scales in the same part of Australia, the effect of land use and land use change (specifically, *Eucalyptus* reforestation) had no impact on streamflow, which was instead mainly driven by climate variability.

These contrasting results from different climatic areas pose serious challenges for land management, especially in small catchments that are often affected by local water resource plans. For example, the consequences of afforestation on streamflow are so important that in South Africa and South Australia tree plantation water use is regulated by the state [*Greenwood*, 2013]. However, it has been recognized that these regulations are based on limited evidence [*Dye*, 2013], and are sometimes guided by simplistic models that are not able to represent the response of catchments to land use changes across different climatic conditions and catchment characteristics [*Greenwood et al*., 2014]. Hydrological models designed for ephemeral catchments are less common than models used for perennial stream systems [e.g., *Viola et al*., 2014], since they need to account for the highly nonlinear response of streamflow to rainfall events and the moisture conditions antecedent to rainfall events [*Ye et al*., 1997, 1998]. Models used in ephemeral catchments are often conceptual, with a limited number of parameters [e.g., *Ye et al*., 1997, 1998; *Viola et al*., 2014], with physically based and spatially distributed models only recently applied to ephemeral catchments [*Camporese et al*., 2014a; *Niedda and Pirastru*, 2014; *Jiang et al*., 2015]. Models of flow duration curves designed for ephemeral streams are also available in the literature [*Viola et al*., 2011; *Pumo et al*., 2014].

Here we present annual water balances from 2011 to 2014 in two ephemeral catchments in south eastern Australia. The study catchments, similar in size and topography, differ in land use, with one catchment a young eucalypt plantation and the other grazing pasture. This study aims to (1) define the importance of groundwater level decline as a result of the recent conversion from pasture to tree plantation, to streamflow using climate, hydrology, and hydrogeology data from both catchments, and (2) corroborate the interpretation of the measurements, especially in terms of overall catchment water balance and generation of streamflow, using the integrated surface–subsurface hydrological model CATchment HYdrology (CATHY). It is hoped this will illuminate the challenges of hydrological monitoring, modeling, and management in ephemeral catchments.

2. Methods

2.1. Site Description

The study area consists of a pair of small, adjacent catchments located in south-western Victoria in south-eastern Australia (−37.39°, 142.39°); one catchment is 0.8 km^2 and is predominantly covered (76% of the catchment area) by a *Eucalyptus globulus* (Blue Gum) plantation established in July 2008, while the other catchment is a 0.5 km^2 farm, mostly pasture for sheep grazing (Figure 1), with a small area of trees (eucalypts, 0.03 km^2). Both catchments are underlain by the same weathered/fractured rock aquifer, the Devonian Dwyer Granite (390–395 Ma) [*Hergt et al*., 2007; *VandenBerg*, 2009]. The upper 10–20 m of the granite is well-weathered, porous and permeable saprolite; below this is relatively fresh, fractured bedrock. The two catchments will be referred to as the eucalypt and pasture catchments, respectively.

Prior to tree planting in July 2008, the eucalypt catchment was predominantly grazing pasture. During planting, this catchment was ripped to an average depth of 800 mm, and mounding was built to an average height of 300 mm. The designed stocking density was 1010 trees per ha (2.2 m between trees along a row, and 4.5 m between rows), and fertilizer was applied to the mounds at 60 kg per ha (R. McEwen, McEwens contracting, personal communication, 2011).The tree rows run east-west in the main north-eastern part of the catchment, and north-south to the west of H Addinsalls Rd. (Figure 1). In surveys taken in 2011, 2013, and 2015, the mean height of trees was 8.9, 11.4, and 13.7 m with the mean diameter at breast height over bark of 9.6, 12.2, and 14.3 cm, respectively; the number of trees per hectare declined from 1139 in 2011 to 889 in 2015 (D. Shelden, Macquarie forestry, personal communication, 2014). The eucalypt catchment understory was periodically grazed by cattle. Both catchments were originally open eucalypt woodland prior to European settlement and conversion to pasture occurred in the late 1800s. There are two small dams in each catchment (10–50 m^2 in area), and the roads at the site are single lane and unsealed. Details on the geology of the two catchments are provided in *Dean et al*. [2015]. The topography of the site (hills in the middle of a broad valley) suggests that both catchments are local groundwater systems, with no regional groundwater inputs (Figure 1).

The climate is Mediterranean or maritime/temperate (Cfb in the Köppen classification); the average annual rainfall for the area since records began in 1902 (Australian Bureau of Meteorology) is 672 mm, and the average annual pan evaporation was estimated at 1315 mm, exceeding rainfall for the majority of the year, excepting the winter months of May through September [*Dean et al*., 2014].

2.2. Monitoring Network

2.2.1. Groundwater and Surface Water

The eucalypt catchment has 10 bores and the pasture catchment has 13 bores drilled to varying depths (Supporting Information Table S1). All of the bores in the eucalypt catchment were drilled in August 2009 except bores E83, E84, and E85, which were installed in the mid-1990s. Two bores in the pasture catchment (P95 and P96) were installed in 2009, while the rest were installed in the late 1980s. Groundwater loggers were installed in every bore in the eucalypt catchment in August 2009, measuring at a minimum 4 h time interval; eight bores in the pasture catchment have a logger measuring at the same frequency (Figure 1). Prior to installation of groundwater loggers in the older bores in both catchments, groundwater levels were generally measured manually every month. There is a V-notch weir at the outlet of each catchment on both creeks, with one bore immediately adjacent to the weir in the eucalypt catchment and two bores next to the pasture catchment weir (Figure 1). The bores adjacent to the weirs have Campbell CS450-L pressure transducers (accuracy ± 0.01 m) measuring water level, temperature and electrical conductivity (EC) at 30

min intervals, while the other bores have Schlumberger Mini Diver loggers (accuracy ± 0.025 m) measuring water level and temperature. At the weirs the surface water level was measured using a standard V notch construction, and EC was logged in the weir pool along with water level at 30 min intervals [*Dresel et al*., 2012]. The weir rating curve was provided by the installation contractor. The minimum water level measured is approximately −0.2 m in local coordinates, relative to the stick gauge in the pool. The minimum level for flow through the weir is 0.1 m; the top of the V notch is at 0.3 m.

A weather station was installed on the ridge between the two catchments where solar radiation, wind speed and direction, relative humidity, ambient temperature, and rainfall were measured at 30 min intervals (Decagon Devices Inc. Em50g). Daily rainfall measurements were also available from an Australian Bureau of Meteorology (BoM) station approximately 2 km south of the study site (station number 089019); these correlated well with onsite rain gauges. Data from the onsite gauges were not used in the water balances or as model inputs due to periodic issues with the instruments. The measured climate parameters were used to calculate vapor pressure deficit (VPD) based on *Allen et al*. [1998].

2.2.2. Sap Flow

Sap flow measurements were used to estimate transpiration, which was then used to assess actual evapotranspiration (ET_a) in the eucalypt catchment. Sap flow was measured using the Edwards Industries HeatPulser setup based on methods described in *Green et al*. [2003] and *Steppe et al*. [2010]; heat-pulse times were recorded on a Campbell Scientific CR1000 logger at 30 min intervals. The Edwards Industries sap flow sensors were installed in three 4 m × 4 m plots within the plantation; the plot sizes were necessarily small due to the presence of young bulls sharing the paddock, and heavy duty fencing had to be installed. Plot 1 was close to the ephemeral drainage line near bores E84/5, Plot 2 halfway up the slope towards the top of the catchment near bore E83, and Plot 3 was installed at the top of the catchment near bore E97; average groundwater levels were at different depths in the three plots (Supporting Information Figure S1).

In early October 2011, one sap flow sensor per tree was installed in four trees in each plot, at a depth of 0.5 cm below the bark. This setup was kept until mid-April 2012, when one sensor in each plot was removed and reinstalled deeper (2.5 cm beneath the bark) into a tree with a shallow sensor already installed. This second setup was designed to take into account variations in sap velocity across the profile of the sap wood, and remained until late September 2012 (except Plot 1, which failed in late May). A third setup involved the installation of four sensors in two new trees in each plot, at different depths in the sapwood (0.5, 1.5, 2.0, and 2.5 cm beneath the bark; Supporting Information Tables S2 and S3). Again, this design was intended to further ensure that variations in sap velocity across the xylem were taken into account, but unfortunately only the setup in Plot 3 worked with this configuration, while the sensors in the other two plots failed. However, there was good agreement in sap flow estimates across all setup configurations indicating that intra- and intertree differences in sap velocity are reasonably accounted for in the transpiration and error estimates. Wood and wound parameters (Supporting Information Table S3) were determined using the methods prescribed in the Edwards Industries HeatPulser manual, following the methodology of *Swanson and Whitfield* [1981] and *Steppe et al*. [2010]. For those trees where wounding and wood parameters were not measured, average values from the entire study period were used.

Transpiration was calculated from 30 min measurement intervals, summed to give daily values, and extrapolated to the entire area of the active xylem in the measured tree to give a flux (volume per area of xylem; where there was more than one sensor per tree, the xylem area used was divided by the number of sensors present). This was then up-scaled to provide fluxes per ha using the tree density of 1010 stems per ha for 2012 (section 2.1). These values were then converted to mm for comparison with the other ET_a estimates. Night time fluxes were assumed to be zero as night time flow is often highly variable and hard to separate from background sap flow using the heat pulse method [*Benyon*, 1999; *Burgess et al*., 2001; *Link et al*., 2014].

ET_a estimates in the eucalypt plantation are based on the sap flow measurements using only data from Plot 3, as this was the longest and most complete set of data, and consistently gave values in between the upper and lower bounds of Plot 2 and Plot 1, respectively; however, data from all the plots is presented here for completeness (Supporting Information Figure S2).

2.2.3. Eddy Covariance

An open path eddy covariance system (IRGASON, Campbell Scientific) was installed in the pasture catchment to measure evapotranspiration from March 2012 to February 2013, providing almost 1 year of ET_a measurements. The system was located in the northeast of the catchment at an elevation of 291 m a.s.l.,

with sensors placed 3.20 m above the ground (Figure 1). The dominant wind direction is from the southeast and thus this setup ensured that pasture dominated the instrument footprint. Wind and water vapor data were collected at a frequency of 10 Hz and subsequently used to estimate hourly evapotranspiration fluxes with the software EddyPro (LI-COR Biosciences, 2012). Hours with significant rainfall were removed because the water droplets interfered with the open path infrared gas analyzer. The evapotranspiration measured using eddy-covariance in the pasture catchment from 16 March 2012 to 29 February 2013 was extrapolated to fit the same time period as the annual water balance (February 2012 to January 2013) by assuming average daily evapotranspiration for the missing days in February and March 2012.

2.3. Water Balance

Water balances were carried out for 4 years (February 2011 to January 2012, February 2012 to January 2013, February 2013 to January 2014, and February 2014 to January 2015) for both catchments using the equation:

$$P = ET_a + Q + \Delta h + GW_{out}, \tag{1}$$

where P is precipitation, ET_a is actual evapotranspiration, Q is runoff (taken as total annual streamflow at the weirs divided by the catchment area), Δh is the change in groundwater storage, and GW_{out} is the outflow of groundwater divided by the catchment area. Accordingly, all values in equation (1) are equivalent water depths (mm). The equation was rearranged to solve for ET_a for comparison with the direct measurements of transpiration from both catchments.

The change in groundwater storage (Δh) was calculated as the average change in water table height in bores in each catchment, multiplied by the specific yield estimated at the study site (0.095 ± 0.014) [*Dean et al*., 2015]. The change in water table height was calculated from the groundwater level loggers by taking the difference in groundwater level from one time-step to the next, and then summing them for the whole year. There was significant barometric noise in the data that could not be removed using traditional methods [e.g., *Toll and Rasmussen*, 2007; *Butler et al*., 2011], because the changes in water level were positively rather than negatively correlated with barometric pressure; therefore, a 15 day moving average of the groundwater level, and a 15 day time step was used to remove the small barometrically forced fluctuations that bear no relationship to rainfall [*Dean et al*., 2015].

Groundwater discharge at the catchment boundary (Q_{out}) was calculated using Darcy's law:

$$Q_{out} = -KiA, \tag{2}$$

where K is the average hydraulic conductivity of the weathered upper 10–20 m of the granite aquifer (discussed below), i is the hydraulic gradient at the downstream end of the catchments, and A is the cross-sectional area of the catchment aquifer at its downstream discharge point. The hydraulic gradient i was calculated as the average difference in water level in bores at the downstream end of the catchment (E93–E90 and P74–P96 in their respective catchments) for each year, divided by the distance between them. The cross-sectional area A, through which groundwater is assumed to flow out of the catchment, was estimated by the width of the catchment at the downstream end, multiplied by the soil depth used in the model simulations (see section 2.4.2; 2500 m^2 in the eucalypt catchment and 1310 m^2 in the pasture catchment); it is possible that heterogeneous fracture flow may occur in the weathered granite aquifer here, but we do not see evidence for this occurring at the catchment outlets defined in this study [*Dean et al*., 2014]. GW_{out} values were then calculated by multiplying Q_{out} by the number of days in each year and dividing by the catchment area to obtain an equivalent depth.

Hydraulic conductivity values were obtained from slug tests that were carried out on six bores by injecting 2 L of water into the well and recording the change in hydraulic head every minute using the already installed groundwater level loggers (Supporting Information Table S1). Hydraulic conductivity (K) was then calculated using *Hvorslev*'s [1951] method:

$$K = \frac{r^2 \ln\left(L_e/r'\right)}{2L_e t_{0.37}}, \tag{3}$$

where r is the radius of the well casing, r' is the radius of the well screen, L_e is the length of the well screen, and $t_{0.37}$ is the time at which the drawdown ratio equals 0.37. The median K value of

the six measurements was then used for both catchments (2.2×10^{-6} m/s; Supporting Information Table S1).

2.4. Integrated Modeling

2.4.1. Model Description

CATHY belongs to the class of recently developed hydrological simulators that resolve in detail the interactions across the land surface–subsurface continuum [*Maxwell et al*., 2014; *Paniconi and Putti*, 2015]. CATHY couples a three-dimensional solver of the Richards equation for subsurface flow in variably saturated soil with a one-dimensional diffusion wave approximation of the de Saint Venant equations for surface water dynamics [*Camporese et al*., 2010].

Rainfall during storm events and potential evapotranspiration during interstorm periods are the main forcings of the model, which partitions these forcings into surface runoff, infiltration, actual evapotranspiration, and changes in storage. In addition to digital terrain data, rainfall and potential evapotranspiration, input for the model includes surface flow parameters, such as Gauckler-Strickler conductance coefficients for hillslopes and channels, and subsurface properties, such as saturated hydraulic conductivity and soil retention curves. To take into account surface roughness and microtopography, surface flow occurs when a minimum water depth (h_{min}) on the surface is exceeded [*Camporese et al*., 2014a]. Overland flow is assumed to concentrate in rills or rivulets confined to hillslope cells, while channel flow occurs on stream cells [*Orlandini and Moretti*, 2009; *Camporese et al*., 2010]. Details of the numerical solutions of the model are in *Paniconi and Putti* [1994] and *Orlandini and Rosso* [1996].

Actual evapotranspiration (ET_a) is computed using a sink term (S) in the Richards equation to account for root water uptake, as in *Camporese et al*. [2015]. Potential transpiration is distributed across the root depth as a function of the root distribution, β, which is expressed as:

$$\beta(z) = \left[1 - \frac{z}{z_m}\right] e^{-\frac{p_z z}{z_m}}, \tag{4}$$

where z is depth (i.e., positive downward), z_m is the maximum rooting depth, and p_z is an empirical shape parameter [*Vrugt et al*., 2001]. Water stress is modeled using a reduction function α dependent on soil moisture θ [*Feddes et al*., 1976]. Accordingly, the reduction function is zero at saturation, when oxygen stress inhibits root water uptake, then α increases linearly up to 1 at the anaerobiosis point (θ_{an}) and the vegetation transpires at its potential rate until soil moisture remains above a certain value associated with incipient water stress (θ_{ref}); when soil moisture falls below θ_{ref}, transpiration reduces linearly until it reaches zero at the wilting point (θ_{wp}).

Using this formulation, the actual root water uptake rate from the ith node along each vertical series of nodes in the three-dimensional grid can be calculated as:

$$S(z_i) = \alpha(\theta_i) \frac{\beta(z_i)\Delta z_i}{\sum_{i=1}^{m} \beta(z_i)\Delta z_i} ET_p, \tag{5}$$

where Δz_i is the layer thickness associated with the ith node, m is the total number of nodes along the vertical direction with depth not exceeding z_m, and ET_p is potential evapotranspiration. This root water uptake model was used in the simulations of both the pasture and eucalypt catchments. We did not distinguish between soil evaporation and transpiration to limit the number of calibration parameters in the model; we also did not account for seasonal cycles in vegetation growth, which occurs especially in the pasture. Root water uptake compensatory mechanisms were not included here, contrasting with *Camporese et al*. [2015].

2.4.2. Simulation Setup

Starting from a 20 m $\times$ 20 m resolution DEM, three-dimensional subsurface grids were constructed for both catchments. Based on geological information (section 2.1), the soil depths for both catchments were limited to 10 m, for a total of 16 vertical discretization layers and the bedrock was assumed parallel to the surface. The vertical discretization is not uniform, with layers progressively coarsening with depth, starting with the thinnest mesh stratum (0.05 m) at the surface, needed to accurately resolve rainfall–runoff–infiltration partitioning. The resulting 3D grids contain 34,153 nodes and 182,880 tetrahedral elements for the eucalypt catchment and 22,066 nodes and 116,160 elements for the pasture.

Table 1. Observed and Modeled Water Balance Parameters From 2010 to 2014, and the Direct Estimates of ET_a From the Sap Flow and Eddy Covariance Measurements[a]

	2011[b]	2012		2013		2014	
	Observed	Observed	Model	Observed	Model	Observed	Model
Eucalypt Catchment							
P	629	577	577	674	674	556	556
Q	23 ± 7	16 ± 6	14	18 ± 6	7	5 ± 2	1
Δh	−69 ± 10	−77 ± 11	−90	−45 ± 7	−32	−111 ± 16	−97
GW_{out}	2 ± 1	2 ± 1	0	2 ± 1	0	2 ± 1	0
$ET_{(calculated)}$	673 ± 18	636 ± 18	653	699 ± 14	699	660 ± 19	652
ET_a (sap flow)		616 ± 75					
Pasture Catchment							
P	629	577	577	674	674	556	556
Q	22 ± 4	22 ± 5	17	22 ± 6	17	7 ± 3	9
Δh	−6 ± 1	−3 ± 1	−5	5 ± 1	40	−36 ± 3	−67
GW_{out}	5 ± 1	6 ± 1	0	5 ± 1	0	5 ± 1	0
$ET_{(calculated)}$	608 ± 6	552 ± 7	565	642 ± 8	620	580 ± 7	614
ET_a (eddy covariance)		534					

[a]All values are in mm.
[b]Calibration year for the model; errors are 1σ (with a minimum of 1 mm), except for the ET_a sap flow values which are the 95% confidence interval, and Δh where they are the maximum change observed in a 15 day interval [see *Dean et al.*, 2015].

We simulated the period from 16 February 2011 to 15 February 2012 for calibration purposes and from 16 February 2012 to 15 February 2015 for validation, to compare measured with simulated streamflow, water table levels, and ET_a for the validated model.

The atmospheric boundary conditions consisted of rainfall as measured by the BoM rain gauge and potential evapotranspiration (ET_p) provided by the SILO database [*Jeffrey et al.*, 2001] according to *Morton* [1983]. Actual evapotranspiration (ET_a) was then calculated by the model depending on the values of Feddes' parameters (θ_{an}, θ_{ref}, θ_{wp}, z_m, and p_z), as described in the previous section. No-flow conditions were assigned to the bottom of the grids and all the lateral boundaries.

The initial conditions for the calibration simulations were generated by running a warm-up period for the previous 10 years (2001–2011), using measured rainfall rates and estimated ET_p fluxes. A warm-up period of 2 years is usually sufficient to obtain a state that is physically realistic and essentially independent of the conditions assigned at the beginning of the warm-up [e.g., *Camporese et al.*, 2014a,b], but in this case we had to account for the land use change that occurred in the eucalypt catchment when the trees were planted in 2008 and the possibility that the related impact could affect the dynamics of the system for several years. For this reason, the warm-up simulation in the plantation was carried out from 2001 to 2008 with root water uptake parameters typical of the pasture, and then from 2008 to 2011 with those typical of a plantation (more details are given in section 3.3). For consistency, a 10 year warm-up period was used also for the pasture, with root water uptake parameters constant in space and time. The pressure head and surface discharge distributions at the end of the warm-up period were then used as initial conditions for the calibration simulations, while the states at the end of the calibration provided the initial conditions for the validation simulations.

2.4.3. Parameter Calibration

Most of the soil parameters needed by the model were estimated from data collected in the field and from the literature. A detailed description of how the parameters were estimated is reported in *Camporese et al.* [2014a]. The only parameters that needed tuning in order to achieve a satisfactory match between simulated and observed states were h_{min} and some of the variables controlling ET_a, i.e., the root water uptake parameters θ_{an}, z_m, and p_z. The parameter values obtained in the calibration are reported and discussed in section 3.3.

3. Results

3.1. Water Balance, Groundwater Storage, and Streamflow

In 2011, 4% of rainfall in the eucalypt catchment was exported via streamflow (Q) and less than 1% was exported via groundwater flow (GW_{out}); the drop in groundwater storage (Δh) was equivalent to 11% of

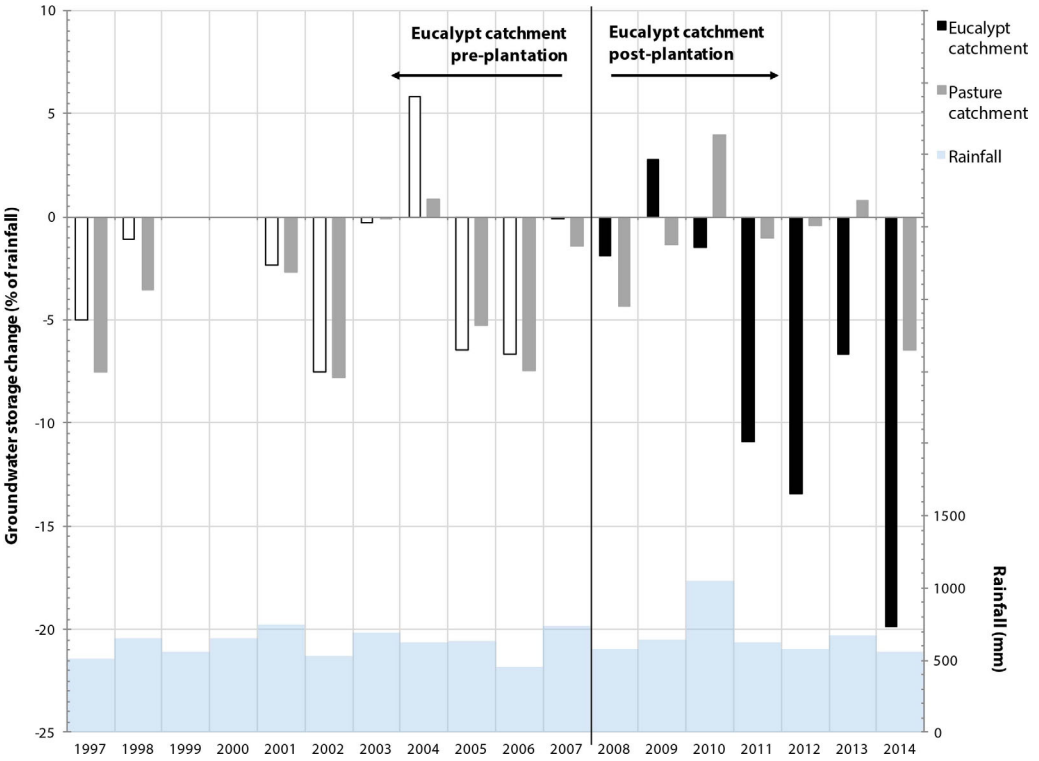

Figure 2. Groundwater storage change (Δh) since the measurements began in both catchments using available data (bi-monthly manual groundwater measurements for bores E83, E84, E85, P74, P75, P80, and P82) back to 1997, and groundwater logger data from late 2009; the hollow bars represent the eucalypt plantation prior to tree planting, and the solid black bars represent the eucalypt catchment after planting. Δh is shown as a percentage of rainfall to normalize the data for comparison (negative values indicates groundwater decline); annual rainfall totals are at the bottom of the figure.

rainfall, and evapotranspiration (ET_{ai}; calculated from the water balance, equation (2)) accounted for *c*. 107% of rainfall (Table 1). In the same year in the pasture catchment, 3% of rainfall was exported via streamflow, 1% by groundwater flow, there was a drop in groundwater storage equivalent to 1% of rainfall, and 97% was calculated to be lost by evapotranspiration (Table 1).

These values were consistent in both catchments for 2012 and 2013. Streamflow accounted for 3–4% of rainfall export in the eucalypt catchment, groundwater export less than 1%, declines in groundwater storage equivalent to 7–13% of rainfall, and calculated evapotranspiration 104–110%. In the pasture catchment, streamflow accounted for 3–4% of rainfall export, groundwater export 1%, groundwater storage changes were equivalent to an increase or decrease of up to 1% of rainfall, and calculated evapotranspiration was 95–97% (Table 1).

In 2014, streamflow in both catchments was about 1% of rainfall (Table 1), significantly lower than the previous years. Groundwater storage decline was 20 and 7% in the eucalypt and pasture catchments, respectively, but groundwater exports remained low at 1% or less in both. This decline in streamflow and groundwater storage relative to rainfall in both catchments resulted in the highest evapotranspiration estimates of 119% of rainfall in the eucalypt catchment and 104% in the pasture (Table 1).

Evapotranspiration calculated from the water balances was consistently greater than rainfall for all years in the eucalypt catchment, explaining the drop in groundwater storage observed in this catchment when compared to the pasture (Figure 2) [*Dean et al*., 2015]. In the pasture catchment, groundwater storage remained stable across the study period, with calculated evapotranspiration less than rainfall every year except 2014. In both catchments, groundwater levels showed seasonal cycles indicating that recharge is still occurring.

The interpretation of streamflow dynamics in ephemeral catchments is complicated because of the combined effects of streamflow rates and flow duration. To compare streamflow in the two catchments, we

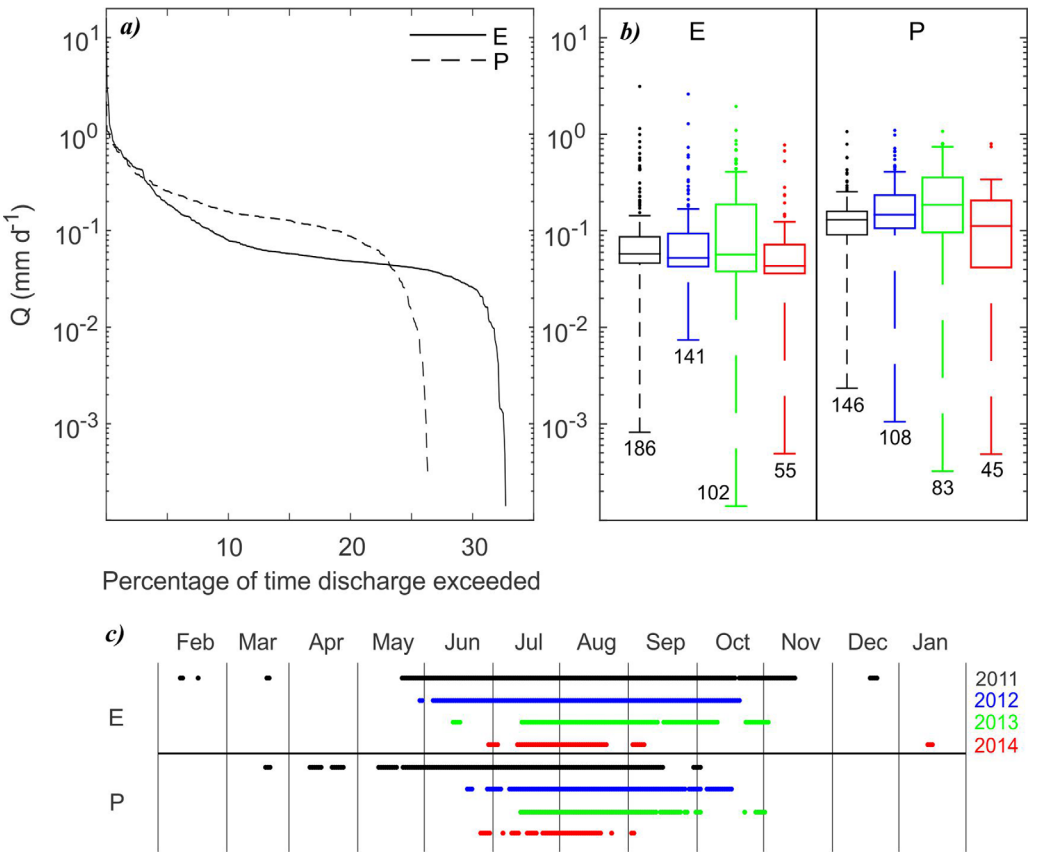

Figure 3. (a) Flow duration curves for the period between February 2011 and January 2015 of daily streamflow for both eucalypt (E) and pasture (P) catchments. (b) Box plots of the flows occurring in different years in the two catchments; the numbers are the days with streamflow in each year. (c) Days within each year when the streams flowed.

used flow duration curves and the statistics of streamflow rates (Figure 3). The eucalypt stream has higher peak runoff and more persistent low flows than the pasture catchment, where the stream commonly flows for a shorter period of the year. The flow rate distributions in the two catchments were statistically different overall (Kolmogorov Smirnov test, $P < 0.05$). The flows also experience variability between years: the distributions of flow in each year in the pasture were statistically different from each other (Kolmogorov Smirnov test, $P < 0.05$); in the eucalypt catchment, streamflow rates in 2011 and 2012, and 2012 and 2013 were of the same distribution (Kolmogorov Smirnov test, $P > 0.05$), while they were statistically different for the remaining years. The streamflow data demonstrates that the slightly lower streamflow rates in the eucalypt catchment were compensated by longer flow duration, such that annual flows in both catchments resulted in similar annual streamflow when compared to annual rainfall.

3.2. Observed Evapotranspiration

Measured transpiration for the trees in the eucalypt catchment for 2012 was 388 ± 20 mm (Supporting Information Table S2). This value excludes interception by the canopy and evaporative losses from the soil, which are estimated to be 44 to $48 \pm 10\%$ of rainfall for south-eastern Australian sites planted with *E. globulus* (1–6 years older than the trees in the current study) and with similar annual rainfall (± 200 mm) [*Benyon et al.*, 2006; *Benyon and Doody*, 2015]. Incorporating this estimate gives a total ET_a for the forested area of 642 ± 78 mm. However, the plantation only covers 76% of the eucalypt catchment, the rest being pasture; the evapotranspiration measured from the pasture catchment (534 mm; see below) was used for the other 24% of the catchment to give a total transpiration from February 2012 to January 2013 of 616 ± 75 mm, very similar to that calculated from the water balance (636 ± 18 mm; Table 1).

The evapotranspiration measured by eddy-covariance in the pasture catchment for 16 March 2012 to 29 February 2013 was 514 mm. This was extrapolated to fit the same time period as the water balance

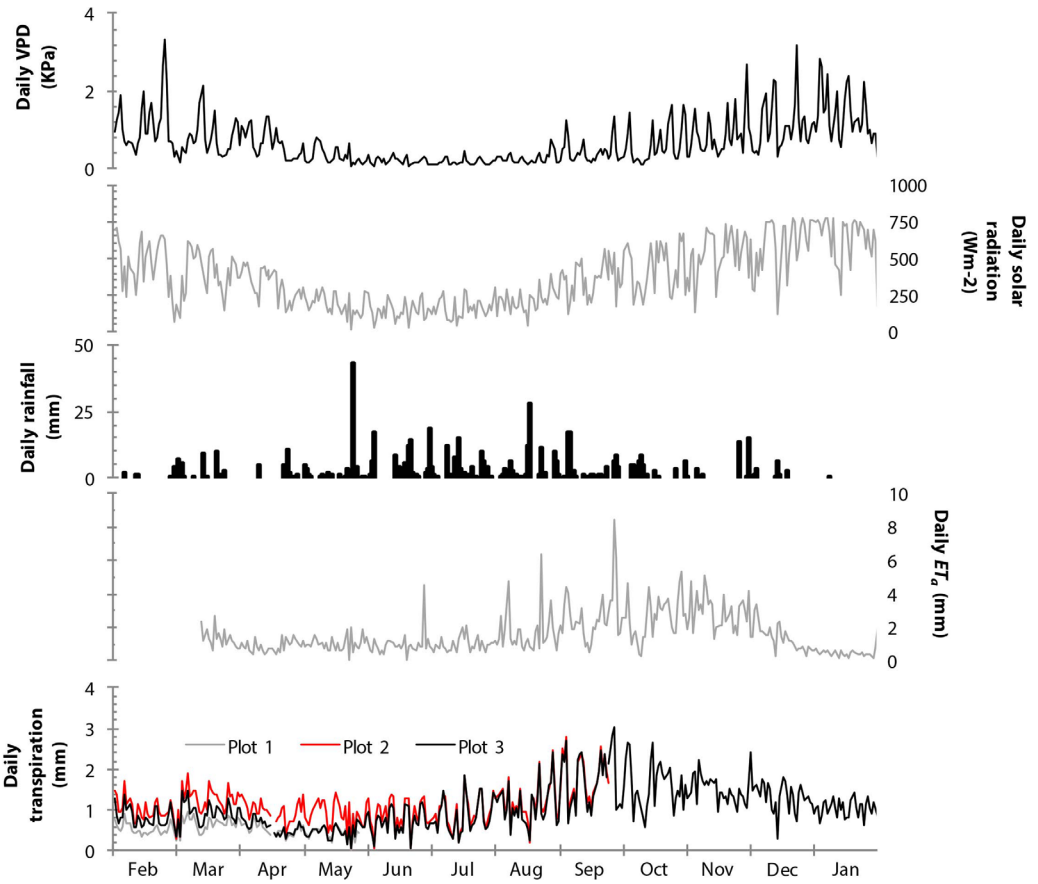

Figure 4. Time series of daily vapor pressure deficit (VPD), daily solar radiation, daily rainfall, daily ET_a from eddy covariance measurements, and daily transpiration from the three sap flow plots.

(February 2012 to January 2013) by assuming average daily evapotranspiration for the missing days in February and March 2012, giving a value of 534 mm, 3% less than that calculated from the water balance (552 $\pm$ 6 mm; Table 1).

Transpiration in the eucalypt catchment and evapotranspiration in the pasture had marked seasonal cycles (Figure 4). They were low early in the year, during and after summer, when the high temperature and the low rainfall reduce the amount of water available for transpiration. In this period of the year, the vegetation cover in the pasture was limited. The rainfall in late autumn and winter provides water for transpiration, which increased in both catchments around July–August, reaching the highest values in the period between September and December, when daily solar radiation and VPD are increasing. This is also the period of vegetation growth in the pasture. Evapotranspiration rates reduced again as summer approached in December because of the lower water availability and the higher temperatures.

Differences in transpiration rates were observed in the three plots in the plantation from February through May, with Plot 1 experiencing the lowest transpiration rates and Plot 2 the largest (Supporting Information Figure S2). The differences in the transpiration rates in Plots 2 and 3 reduced in late autumn/early winter, when rainfall started replenishing the unsaturated zone. These results agree with the accessibility of trees to groundwater, as shown in Figure 1. In Plot 1, the groundwater is well within the average rooting depth of Blue Gums (6–8 m) [*Benyon et al.*, 2006]. However, the access to groundwater in this part of the catchment might be a partly limiting factor due to the high salinity (5000–10,000 μS cm^{-1}; Supporting Information Table S2); this would explain the lower sap flow rates in Plot 1. Despite the high salinity, in the lower parts of the catchment the drop in groundwater storage is greatest. This means that while the trees may preferentially extract fresh water from the unsaturated zone, transpiration appears to also be partially sourced from groundwater in this part of the catchment. In Plot 2, the depths to groundwater are deeper, but still

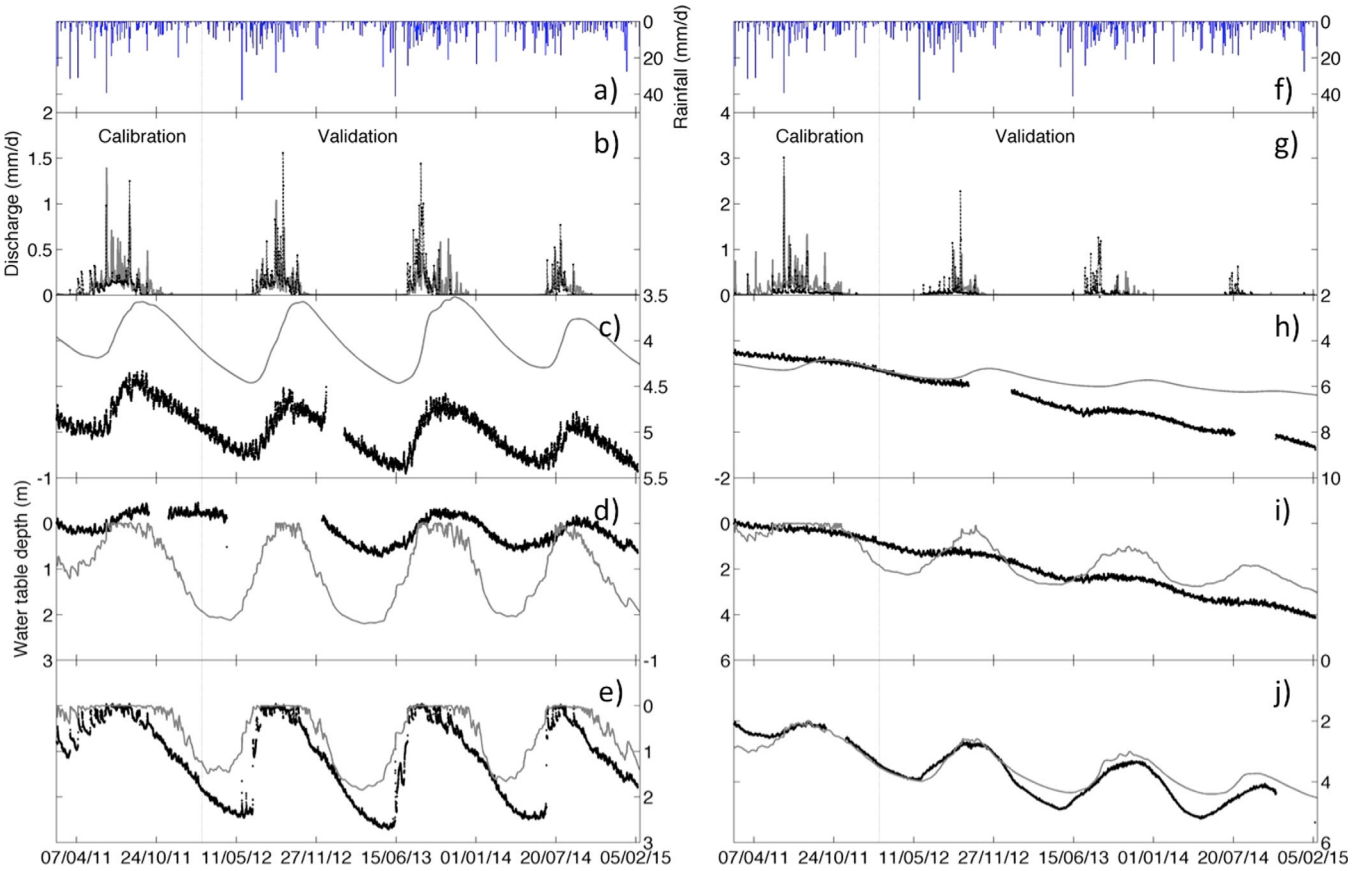

Figure 5. Comparison between observations and CATHY simulation results for the calibration (16 February 2011 to 15 February 2012) and validation periods (16 February 2012 to 15 February 2015): daily streamflow in the (b) pasture and (g) eucalypt catchments. Water table levels in boreholes (c) P74, (d) P76, (e) P96, (h) E83, (i) E84, and (j) E90; note that the *y* axis title of Figure 5d applies to all the water level figures. Black dots and lines refer to observations and gray lines indicate simulation results. Daily rainfall is reported in Figures 5a and 5f.

within reach of the root system; the access to this additional pool of water would explain the largest sap flow rates in this plot. In the upper parts of the catchment (i.e., Plot 3), where the groundwater is too deep for the trees to directly access (Figure 1), sap flow rates were lower in the dry summer, but matched those in Plot 2 as water became available with the first rain in March–April.

3.3. Model Calibration and Validation

A manual calibration of the model was performed to achieve a satisfactory match between observed and simulated daily streamflow and water table. Accordingly, the minimum ponding head (h_{min}) was assigned a value of 5.0×10^{-6} m for the eucalypt catchment and 4.0×10^{-4} m for the pasture; the much smaller value found for the eucalypt catchment is probably needed to compensate for the tree furrows, which hinder the retarding effect of microtopography on surface runoff and could not be included in the surface representation due to the DEM resolution. In both catchments, we assigned $\theta_{ref} = 0.16$ and $\theta_{wp} = 0.056$, computed from the model ψ–θ retention curve as the corresponding values to pressure heads of -4 and -150 m, respectively, as suggested by *Feddes et al.* [1976]. In order to take the root growth into account, the maximum rooting depth z_m in the eucalypt catchment was assumed to increase linearly with time, according to the relationship $z_m = 0.8515 + 0.4515\ t$, where t is time in years from planting and the coefficients were computed based on a constant ratio between root and above-ground biomass [*Fabião et al.*, 1995] and the available tree height data. Therefore, the final value of z_m at the end of the validation simulation was approximately 4 m, while maximum root depths of mature *E. globulus* were reported between 6 and 8 m [*Benyon et al.*, 2006]. The root water uptake parameters left to tune were θ_{an} and p_z in both catchments and z_m in the pasture. Values of $\theta_{an} = 0.38$ and $p_z = 0.095$ were assigned to the eucalypt catchment, whereas $\theta_{an} = 0.40$ (i.e., no oxygen stress), $z_m = 1.0$ m, and $p_z = 4.025$ were found for the pasture catchment. As p_z is constant in space in the current model implementation, z_m equal to 0.5 m was assigned in the eucalypt

catchment to the areas not covered by trees, to obtain a root distribution similar to the one used in the pasture. All the model parameters are summarized in Supporting Information Table S4. Although hydraulic conductivity was not tuned, it was assumed to be slightly larger than the estimates reported in Supporting Information Table S1 (2.31×10^{-7} to 3.36×10^{-6} m s^{-1}) because slug tests are known to underestimate K [*Butler and Healey*, 1998].

By tuning only h_{min} and some of the Feddes' parameters, the model adequately reproduced the magnitude and timing of daily streamflow for the calibration period (Figure 5), with Willmott indexes of agreements (*IoA*) [*Willmott*, 1981] for the eucalypt and pasture catchments of 0.83 and 0.79, respectively. For the validation period, model performance was still satisfactory for the pasture catchment ($IoA = 0.72$), whereas streamflow prediction in the eucalypt catchment degraded significantly ($IoA = 0.37$) (Figure 5); the first streamflow peaks of the wet season being, in general, not well reproduced by the simulations. This was probably due to uncertainties in the definition of the bedrock geometry, parameter spatial variability not accounted for in the model, or changes in soil parameters of the first 0.8 m caused by tree planting (section 2.1). Nevertheless, given that streamflow accounts for no more than 3–4% of the total annual precipitation in both catchments, the modeling results can be considered acceptable, and flow seasonality, typical of ephemeral streams, was well captured.

Overall, the model was able to reproduce the observed water table dynamics in the shallowest bores (i.e., E83, E84, and E90 in the eucalypt catchment; P74, P76, and P96 in the pasture). During the calibration period (Figure 5), the match was particularly good for the bores close to the outlets, i.e., P96 and E90, with *IoA*s of 0.72 and 0.85, respectively, and coefficients of determination (R^2) of 0.74 and 0.67. On the eucalypt catchment hillslope (E83), the model struggled to reproduce the correct dynamics ($IoA = 0.35$ and $R^2 = 0.06$), probably due to some spatial variability of the hydraulic conductivity that was not captured in this study. However, on the pasture hillslope (P74), the groundwater dynamics were generally well captured by the model ($R^2 = 0.84$), although the absolute values of the measured water table levels were not as well matched ($IoA = 0.32$), probably due to some variabililty in the soil thickness, not accounted for in the model, and/or possible leakages to underlying geological formations, whereas we assumed a perfectly impermeable bedrock. The model performance was still reasonable, but poorer compared to E90 and P96, for the bores E84 ($IoA = 0.66$ and $R^2 = 0.37$) and P76 ($IoA = 0.30$ and $R^2 = 0.34$), located close to the creeks, but further upstream. This was likely caused by the dynamics of the water table here, which exhibits behavior suggestive of a periodically confined aquifer [*Dean et al*., 2015].

An overall satisfactory model performance was also achieved for the water table in the validation phase (Figure 5). Again, the best model performance was achieved for the bores close to the outlets ($IoA = 0.89$ and $R^2 = 0.87$ for E90; $IoA = 0.79$ and $R^2 = 0.72$ for P96), while the overall dynamics was captured not only in P74 ($IoA = 0.31$ and $R^2 = 0.71$), but also in E83 ($IoA = 0.56$ and $R^2 = 0.85$). Consistent with the calibration phase, the model partially failed to reproduce the water levels in E84 ($IoA = 0.66$ and $R^2 = 0.30$) and P76 ($IoA = 0.36$ and $R^2 = 0.36$), with simulated water table fluctuations significantly overestimated compared to the observed ones.

Potential evapotranspiration, ET_p (calculated from the Morton's formula), was used as a forcing input to the model, and is converted into ET_a by means of the root water uptake model. The total cumulative annual evapotranspiration simulated in the pasture and eucalypt catchments compared well with the estimates from the water budget and measurements obtained by the eddy covariance system and sap flow data (section 3.1 and Table 1).

4. Discussion

The most surprising result from the 4 years of monitoring data is that the streams in both catchments have similar annual runoff totals despite the change in land use that has had a pronounced effect on groundwater levels.

In the years prior to 2008 the changes in groundwater storage in the two catchments were generally well matched (Figure 2). In 2009, there is a slight increase in groundwater storage in the eucalypt catchment, likely caused by the low ET_a of the immature trees and enhanced recharge down the freshly dug furrows from tree planting the previous year. From 2010 the groundwater levels in the eucalypt catchment declined

sharply compared to only small declines or even gains in the pasture catchment (Figure 2). The timing of the decline in groundwater levels in the eucalypt catchment confirms that this is not an artifact of some other factor differentiating the two study catchments (e.g., geology), but is mainly due to the establishment of the plantation and the associated increase in evapotranspiration. Both the water balances and the model agree that ET_a in the eucalypt catchment is greater than in the pasture, and this was also verified by the sap flow and eddy covariance ET_a measurements from 2012 (Table 1).

The water balance terms given by the simulations are consistent with the estimates derived from the observations. In particular, the model was able to quantify the changes in total catchment water storage, including the unsaturated zone, which would be impossible to estimate by the water table data only. Furthermore, in the eucalypt catchment, it was possible to correctly identify these storage changes only be considering the root growth dynamics, albeit with a simple conceptualization.

Annual ET_a in the study plantation (636–699 mm) is less than the average ET_a in South African eucalypt plantations of 1100–1200 mm [*Dye and Versfeld*, 2007], and is in the lower range of other estimates from south-eastern Australia (488–1343 mm) [*Benyon et al*., 2006; *Benyon and Doody*, 2015]. In South Africa, ET_a was limited mainly by rainfall, whereas in south-eastern Australia groundwater utilization was shown to be the primary driver of plantation transpiration [*Benyon et al*., 2006; *Benyon and Doody*, 2015]. In the present study, groundwater is a source of water uptake by the trees in parts of the catchment, while the limited runoff interception and subsequent utilization by the trees, along with the groundwater salinity (see section 3.2), may be keeping ET_a in the lower bounds of values observed in other studies.

Notwithstanding the large drop in groundwater levels in the eucalypt catchment, annual streamflow was similar to the pasture catchment, although there are indications that the trees may be having some impact on streamflow. Streamflow rate distributions in the eucalypt catchment were not significantly different from 2011 to 2013, but were different in 2014. This may be evidence of the trees impacting streamflow; however, rainfall in 2014 was very low, thereby possibly causing this change in and of itself, or magnifying the impact of the trees. Overall, flow distributions were significantly different between the two catchments as well, with the eucalypt catchment usually generating lower streamflow rates, but with periods of flow lasting longer than in the pasture catchment (Figure 3); this resulted in similar annual streamflow values (Table 1). The longer flow durations in the eucalypt catchment may be due to contributions from groundwater discharge into the stream channel [*Dean et al*., 2015], and if groundwater levels continue to decline this may eventually result in a decrease in overall streamflow in this catchment. This is also indicated by the model, which underestimated streamflow in the eucalypt catchment for 2014, due to a slow but steady decline in return flow (i.e., groundwater fluxes from the subsurface to the surface). By comparison, the simulation results do not exhibit such decrease of return flow in the pasture catchment (Supporting Information Figure S3).

To try to understand in simple terms the relationship between the rainfall regime in the two catchments and streamflow, we compared the relationship between annual rainfall and the percentage of rainfall that became runoff in different years (Figure 6a). The ratio of annual runoff and rainfall was very similar in the two catchments and in 2014 was visibly lower than 2012 even though the annual rainfall was similar in these 2 years. Since the flow is intermittent, the rainfall regime may be as important as the total annual rainfall. This is clearly shown in Figures 6b and 6c, where it appears that the rainfall frequency λ (i.e., the number of days in the year with rainfall divided by the number of days in the year), is strongly affecting the streamflow in both catchments, while the variability in the average daily rainfall amount α (i.e., the annual rainfall depth divided by the number of rainy days in the year), appears less important. One interpretation of these results is that the gradient of the catchment slopes (and downslope orientation of the tree furrows in the eucalypt catchment, see below) directly induces streamflow during rainfall events, and for at least part of the year are disconnected from groundwater, which is able to feed the two streams only in the wetter part of the year. Frequent rainfall events would keep the catchment surface relatively wet, therefore encouraging wetness connectivity that has been found to be a key driver of runoff generation in many experimental hillslopes and catchments [e.g., *McDonnell*, 2013]. The drop of rainfall frequency below a certain threshold, which appears to be about 0.32 day in the study catchments, caused a sharp reduction of streamflow. This also reinforces the critical importance of antecedent catchment storage conditions prior to a given rainfall event in driving streamflow in ephemeral catchments, as documented in previous studies [e.g., *Ye et al*., 1997; *Viola et al*., 2014; *Niedda and Pirastru*, 2014].

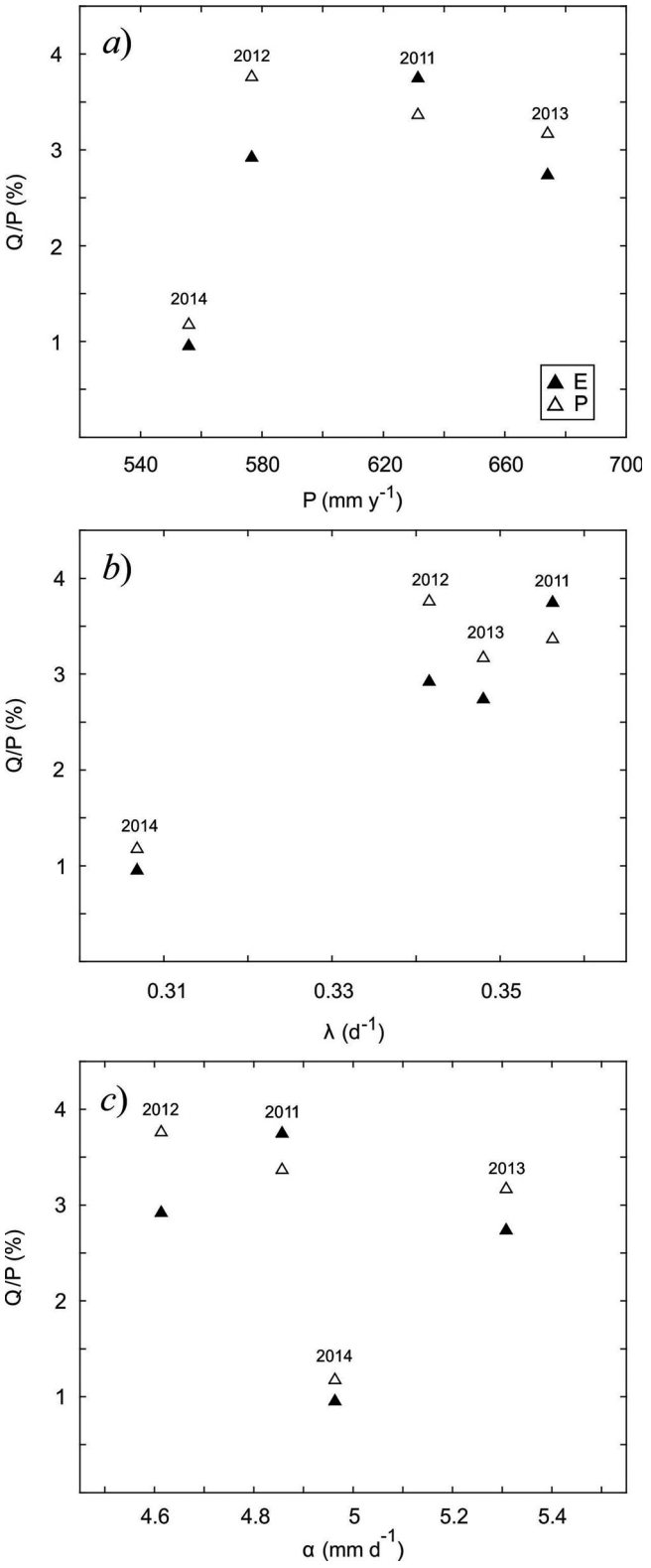

Figure 6. Relationship between the ratio of annual streamflow and the percentage of rainfall with (a) annual rainfall, (b) frequency of rainfall occurrence λ, and (c) average daily rainfall amount in a year, α, in the eucalypt (E, closed symbols) and pasture (P, open symbols) catchments.

Furthermore, the furrows dug to plant the trees run downslope over the majority of the catchment (Figure 1), facilitating overland flow toward the stream channel. The trees are planted in the mound created by the furrows, thereby allowing the furrows themselves to act as rapid conduits for runoff downslope. This was somewhat corroborated by the model: to achieve accurate representations of the streamflow in the eucalypt catchment with CATHY, the minimum ponding head (h_{min}) values (i.e., the threshold that must be crossed in order to generate runoff) were *c*. 100 times smaller than in the pasture catchment (5.0×10^{-6} m versus 4.0×10^{-4} m, respectively; Supporting Information Table S4). The greater root water uptake of the eucalypts is offset by the lower h_{min} values in this catchment, which allows runoff and subsequent streamflow to be generated more readily. Therefore, the furrows play an important role in funneling runoff into the stream channel in the eucalypt catchment. Running tree furrows downslope is now common practice in Australia for safety reasons during tree felling, and the evidence presented here indicates that it can also have a positive response for maintaining streamflow in ephemeral catchments.

The limited change in streamflow after such a significant land use change at the study site highlights the region-specific nature of impacts of land use change in semiarid and arid areas. In a parallel study in south-western Victoria, Australia, a tree plantation was shown to decrease streamflow by 55% [*Adelana et al*., 2014]; here the topography was less steep and runoff readily infiltrated into the soil and was intercepted by the trees. Other studies have shown similar streamflow reductions of 50–80% [*Vertessy et al*., 2001; *Benyon et al*., 2009; *Prosser and Walker*, 2009]. However, *Brown et al*. [2005] suggest that it may take more than 5 years following a change in land use for a system to reach a new equilibrium, and further monitoring at the

study site is needed to assess whether a significant decline in streamflow has been delayed or prevented altogether.

This finding is critical for water resources management, because it shows that land use might not be the most important driver of the water balance in small ephemeral catchments, where the interplay of climate, geology, topography (including tree furrows), and land cover determine the dynamics of water fluxes and storage in the catchments. Although the establishment of the plantation has reduced the availability of the groundwater resource within the catchment, as observed elsewhere [*Adelana et al*., 2014; *Benyon et al*., 2006], the water available at the outlet of the catchment did not vary much compared to the adjacent pasture. This is likely due to the combination of topography and tree furrows, which allows water from rainfall events to quickly runoff, depending more on the frequency of rainfall occurrence than the amount of rain.

Additionally, the results from the monitoring show that the use of hydrologic models to support the development of water management plans need to be carefully considered. Most of the distributed models are commonly calibrated and validated against streamflow; however, in the case of ephemeral catchments the calibration and validation should be carried out considering both streamflow and groundwater levels, to fully describe the dynamics within the catchments. As already suggested by *Ye et al*. [1997], the period of flow and streamflow rates as well as groundwater dynamics are important dynamics that models should be able to describe in ephemeral catchments. As in other studies [*Niedda and Pirastru*, 2014], the model CATHY, with the calibration of few parameters, was able to reproduce the dynamics of groundwater levels, but the simulation of the depth to water table was more challenging for bores further upstream from the catchment outlet. Additionally, the description of topography and bedrock was limited by the availability and resolution of data, thus preventing us from accurately reproducing the tree furrows and wetness connectivity. Accordingly, we conclude that distributed models like CATHY can be effectively used to capture the dynamics of streamflow and groundwater levels in ephemeral catchments; however, to improve model performance in these catchments, where the annual streamflow is very small compared to the other terms of the water balance, there needs to be a detailed and realistic representation of the topography and bedrock geology.

5. Conclusions

Human-induced land use change has the potential to greatly impact hydrological processes at all scales within a catchment. Maintaining streamflow at the outlet is thus a vital part of water management, particularly in arid and semiarid regions. This research provides a comprehensive hydrologic data set over a multiyear period in two catchments situated in a region where annual rainfall is (apart from a few exceptional years) consistently below 800 mm and exceeded by evapotranspiration for much of the year. The multiyear water balances (2011–2014), estimated from the observations and corroborated by the model results, show that in the context of nearly 30 years of groundwater level monitoring at the study site, the recent tree plantation has caused a dramatic decline in groundwater storage compared to the previous land cover of pasture for grazing. However, the tree plantation has had little effect on streamflow. Streamflow in the tree plantation is probably sustained by a combination of wetness connectivity paths, linked to the bedrock geology, and by the downslope orientation of the tree furrows. This hypothesis needs to be further investigated by means of hyper-resolution model simulations that include a detailed representation of the surface topography and bedrock geology. Additionally, further monitoring is needed to determine whether streamflow will reduce as the plantation grows to maturity, or whether the effect shown here can be used to manage tree plantations at a regional scale to minimize plantation impacts on streamflow.

Acknowledgments
This work has been funded by the Australian Research Council and the National Water Commission through Program 4 of the National Centre for Groundwater Research and Training. The authors thank Phil Cook, Peter Hekmeijer, Mark Holmberg, and Michael Adelana of the Victorian Department of Economic Development, Jobs, Transport and Resources, John Collopy and Richard Benyon of The University of Melbourne for their assistance with the sap flow measurements, David Lockington of The University of Queensland for the use of the eddy-covariance equipment, and the landowners, Marcia Field and Macquarie Bank Foundation, for granting access to their land. The data used in this study is available from the Victorian Department of Economic Development, Jobs, Transport and Resources data repository by contacting P.E.D. (evan.dresel@ecodev.vic.gov.au). We also thank the editors and three anonymous referees for their comments that helped significantly improve this manuscript.

References

Adelana, S. M., P. E. Dresel, P. Hekmeijer, H. Zydor, J. A. Webb, M. Reynolds, and M. Ryan (2014), A comparison of streamflow, salt and water balances in adjacent farmland and forest catchments in south-western Victoria, Australia, *Hydrol. Processes*, *29*(6), 1630–1643.

Allen, R. G., L. S. Pereira, D. Raes, and M. Smith (1998), *Crop Evapotranspiration—Guidelines for Computing Water Requirements*, *Irrigation and Drainage Paper 56*, Food and Agric. Organ. of the U.N., Rome.

Benyon, R. G. (1999), Nighttime water use in an irrigated *Eucalyptus grandis* plantation, *Tree Physiol.*, *19*, 853–859.

Benyon, R. G., and T. M. Doody (2015), Comparison of interception, forest floor evaporation and transpiration in *Pinus radiata* and *Eucalyptus globulus* plantations, *Hydrol. Processes*, *29*(6), 1173–1187.

Benyon, R. G., S. Theiveyanathan, and T. M. Doody (2006), Impacts of tree plantations on groundwater in south-eastern Australia, *Aust. J. Bot.*, *54*(2), 181–192.

Benyon, R. G., T. M. Doody, S. Theiveyanathan, and V. Koul (2009), Plantation forest water use in southwest Victoria, *Proj. PNC064-0607*, 103 pp., For. and Wood Prod. Aust., Melbourne, Australia.
Brown, A. E., L. Zhang, T. A. McMahon, A. W. Western, and R. A. Vertessy (2005), A review of paired catchment studies for determining changes in water yield resulting from alterations in vegetation, *J. Hydrol.*, *310*, 28–61.
Brown, S. C., V. L. Versace, R. E. Lester, and M. T. Walter (2015), Assessing the impact of drought and forestry on streamflows in south-eastern Australia using a physically based hydrological model, *Environ. Earth Sci.*, *74*, 6047–6063.
Burgess, S. S. O., M. A. Adams, N. C. Turner, D. A. White, and C. K. Ong (2001), Tree roots: Conduits for deep recharge of soil water, *Oecologia*, *126*(2), 158–165.
Butler, J. J., and J. M. Healey (1998), Relationship between pumping-test and slug-test parameters: Scale effect or artifact?, *Groundwater*, *36*, 305–312.
Butler, J. J., W. Jin, G. A. Mohammed, and E. C. Reboulet (2011), New insights from well responses to fluctuations in barometric pressure, *Ground Water*, *49*, 525–533.
Camporese, M., C. Paniconi, M. Putti, and S. Orlandini (2010), Surface-subsurface flow modeling with path-based runoff routing, boundary condition-based coupling, and assimilation of multisource observation data, *Water Resour. Res.*, *46*, W02512, doi:10.1029/2008WR007536.
Camporese, M., E. Daly, P. E. Dresel, and J. A. Webb (2014a), Simplified modeling of catchment-scale evapotranspiration via boundary condition switching, *Adv. Water Resour.*, *69*, 95–105.
Camporese, M., D. Penna, M. Borga, and C. Paniconi (2014b), A field and modeling study of nonlinear storage-discharge dynamics for an Alpine headwater catchment, *Water Resour. Res.*, *50*, 806–822, doi:10.1002/2013WR013604.
Camporese, M., E. Daly, and C. Paniconi (2015), Catchment-scale Richards equation-based modeling of evapotranspiration via boundary condition switching and root water uptake schemes, *Water Resour. Res.*, *51*, 5756–5771, doi:10.1002/2015WR017139.
Chiverton, A., J. Hannaford, I. Holman, R. Corstanje, C. Prudhomme, J. Bloomfield, and T. M. Hess (2015), Which catchment characteristics control the temporal dependence structure of daily river flows?, *Hydrol. Processes*, *29*(6), 1353–1369.
Dean, J. F., J. A. Webb, G. E. Jacobsen, R. Chisari, and P. E. Dresel (2014), Biomass uptake and fire controls on groundwater solute evolution on a southeast Australian granite: Aboriginal land management hypothesis, *Biogeosciences*, *11*, 4099–4114.
Dean, J. F., J. A. Webb, G. E. Jacobsen, R. Chisari, and P. E. Dresel (2015), A groundwater recharge perspective on locating tree plantations within low-rainfall catchments to limit water resources losses. *Hydrol. Earth Syst. Sci.*, *19*, 1107–1123.
Dresel, P. E., P. Hekmeijer, J. F. Dean, W. Harvey, J. A. Webb, and P. Cook (2012), Use of laser-scan technology to analyse topography and flow in a weir pool, *Hydrol. Earth Syst. Sci.*, *16*, 2703–2708.
Dye, P. (2013), A review of changing perspectives on *Eucalyptus* water-use in South Africa, *For. Ecol. Manage.*, *301*, 51–57.
Dye, P., and D. Versfeld (2007), Managing the hydrological impacts of South African plantation forests: An overview, *For. Ecol. Manage. 251*, 121–128.
Engel, V., E. G. Jobbágy, M. Stieglitz, M. Williams, and R. B. Jackson (2005), Hydrological consequences of Eucalyptus afforestation in the Argentine Pampas, *Water Resour. Res.*, *41*, W10409, doi:10.1029/2004WR003761.
Fabião, A., M. Madeira, E. Steen, T. Kätterer, C. Ribeiro, and C. Araújo (1995), Development of root biomass in an *Eucalyptus globulus* plantation under different water and nutrient regimes, *Plant Soil*, *168*(1), 215–223.
Famiglietti, J. S. (2014), The global groundwater crisis, *Nat. Clim. Change*, *4*, 945–948.
Farley, K. A., E. G. Jobbagy, and R. B. Jackson (2005), Effects of afforestation on water yield: A global synthesis with implications for policy, *Global Change Biol.*, *11*(10), 1565–1576.
Feddes, R. A., P. Kowalik, K. Kolinska-Malinka, and H. Zaradny (1976), Simulation of field water uptake by plants using a soil water dependent root extraction function, *J. Hydrol.*, *31*, 13–26.
Feikema, P. M., J. D. Morris, and L. D. Connell (2010), The water balance and water sources of a Eucalyptus plantation over shallow saline groundwater, *Plant Soil*, *332*(1), 429–449.
Foley, J. A., et al. (2005), Global consequences of land use, *Science*, *309*(5734), 570–574.
Green, S., B. Clothier, and B. Jardine (2003), Theory and practical application of heat pulse to measure sap flow, *Agron. J.*, *95*, 1371–1379.
Greenwood, A. J. B. (2013), The first stages of Australian forest water regulation: National reform and regional implementation, *Environ. Sci. Policy*, *29*, 124–136.
Greenwood, A. J. B., G. Schoups, E. P. Campbell, and P. N. J. Lane (2014), Bayesian scrutiny of simple rainfall-runoff models used in forest water management, *J. Hydrol.*, *512*, 344–365.
Hergt, J, J. Woodhead, and A. Schofield (2007), A-type magmatism in the Western Lachlan Fold Belt? A study of granites and rhyolites from the Grampians region, Western Victoria, *Lithos*, *97*, 122–139.
Hvorslev, M. J. (1951), Time lag and soil permeability in ground water observations, *Bulletin 36*, U.S. Army Waterw. Exp. Stn., Vicksberg, Miss.
Jackson, R. B., E. G. Jobbágy, R. Avissar, S. B. Roy, D. J. Barrett, C. W. Cook, K. A. Farley, D. C. Le Maitre, B. A. McCarl, and B. C. Murray (2005), Trading water for carbon with biological carbon sequestration, *Science*, *310*(5756), 1944–1947.
Jackson, R. B., E. G. Jobbagy, and M. D. Nosetto (2009), Ecohydrology in a human-dominated landscape, *Ecohydrology*, *2*(3), 383–389.
Jeffrey, S. J., J. O. Carter, K. B. Moodie, and A. R. Beswick (2001), Using spatial interpolation to construct a comprehensive archive of Australian climate data, *Environ. Modell. Softw.*, *16/4*, 309–330.
Jiang, Y., X. Xu, Q. Huang, Z. Huo, and G. Huang (2015), Assessment of irrigation performance and water productivity in irrigated areas of the middle Heihe River basin using a distributed agro-hydrological model, *Agric. Water Manage.*, *147*, 67–81.
Link, P., K. Simonin, H. Maness, J. Oshun, T. Dawson, and I. Fung (2014), Species differences in the seasonality of evergreen tree transpiration in a Mediterranean climate: Analysis on multiyear, half-hourly sap flow observations, *Water Resour. Res.*, *50*, 1869–1894, doi:10.1002/2013WR014023.
Maxwell, R. M., et al. (2014), Surface-subsurface model intercomparison: A first set of benchmark results to diagnose integrated hydrology and feedbacks, *Water Resour. Res.*, *50*, 1531–1549, doi:10.1002/2013WR013725.
McDonnell, J. J. (2013), Are all runoff processes the same?, *Hydrol. Processes*, *27*, 4103–4111.
Morton, F. I. (1983), Operational estimates of areal evapotranspiration and their significance to the science and practice of hydrology, *J. Hydrol.*, *66*, 1–76.
Niedda, M., and M. Pirastru (2014) Field investigation and modelling of coupled stream discharge and shallow water-table dynamics in a small Mediterranean catchment (Sardinia), *Hydrol. Processes*, *28*(21), 5423–5435.
Nosetto, M. D., E. G. Jobbagy, A. B. Brizuela, and R. B. Jackson (2012), The hydrologic consequences of land cover change in central Argentina, *Agric. Ecosyst. Environ.*, *154*, 2–11.
Orlandini, S., and R. Rosso (1996), Diffusion wave modeling of distributed catchment dynamics, *J. Hydraul. Eng.*, *1*(3), 103–113.

Orlandini, S., and G. Moretti (2009), Determination of surface flow paths from gridded elevation data, *Water Resour. Res.*, *45*, W03417, doi:10.1029/2008WR007099.
Paniconi, C., and M. Putti (1994), A comparison of Picard and Newton iteration in the numerical solution of multidimensional variably saturated flow problems, *Water Resour. Res.*, *30*(12), 3357–3374.
Paniconi, C., and M. Putti (2015), Physically based modeling in catchment hydrology at 50: Survey and outlook, *Water Resour. Res.*, *51*, 7090–7129, doi:10.1002/2015WR017780.
Prosser, I. P., and G. R. Walker (2009), A review of plantations as water intercepting land use in South Australia, in *Water for a Healthy Country National Research Flagship*, *Rep. 33*, CSIRO, Tantanoola, SA, Australia.
Pumo, D., F. Viola, G. La Loggia, and L. V. Noto (2014), Annual flow duration curves assessment in ephemeral small basins, *J. Hydrol.*, *519*, 258–270.
Smakhtin, V. U. (2001), Low flow hydrology: A review, *J. Hydrol.*, *240*(3–4), 147–186.
Snyder, K. A., and D. G. Williams (2000), Water sources used by riparian trees varies among stream types on the San Pedro River, Arizona, *Agric. For. Meteorol.*, *105*(1–3), 227–240.
Steppe, K., D. J. W. De Pauw, T. M. Doody, and R. O. Teskey (2010), A comparison of sap flux density using thermal dissipation, heat pulse velocity and heat field deformation methods, *Agric. For. Meterol.*, *150*, 1046–1056.
Sterling, S. M., A. Ducharne, and J. Polcher (2012), The impact of global land-cover change on the terrestrial water cycle, *Nat. Clim. Change*, *3*, 385–390.
Swanson, R. H., and D. W. A. Whitfield (1981), A numerical analysis of heat-pulse velocity theory and practice, *J. Exp. Bot.*, *32*, 221–239.
Toll, N. J., and T. C. Rasmussen (2007), Removal of barometric pressure effects and earth tides from observed water levels, *Ground Water*, *45*, 101–105.
VandenBerg, A. H. M. (2009), Rock unit names in western Victoria—Seamless geology project, *Geol. Surv. Vic. Rep. 130*, State Gov. of Vic., Australia.
Vertessy, R. A., F. G. R. Watson, and S. K. O'Sullivan (2001), Factors determining relations between stand age and catchment water yield in mountain ash forests, *For. Ecol. Manage.*, *143*, 13–26.
Viola, F., L. V. Noto, M. Cannarozzo, and G. La Loggia (2011), Regional flow duration curves for ungauged sites in Sicily, *Hydrol. Earth Syst. Sci.*, *15*(1), 323–331.
Viola, F., D. Pumo, and L. V. Noto (2014), EHSM: A conceptual ecohydrological model for daily streamflow simulation, *Hydrol. Processes*, *28*(9), 3361–3372.
Vrugt, J. A., M. T. vanWijk, J. W. Hopmans, and J. Šimůnek (2001), One-, two-, and three-dimensional root water uptake functions for transient modeling, *Water Resour. Res.*, *37*(10), 2457–2470.
Willmott, C. J. (1981), On the validation of models, *Phys. Geogr.*, *2*(2), 184–194.
Ye, W., B. C. Bates, N. R. Viney, M. Sivapalan, and A. J. Jakeman (1997), Performance of conceptual rainfall-runoff models in low-yielding ephemeral catchments, *Water Resour. Res.*, *33*(1), 153–166.
Ye, W., A. J. Jakeman, and P. C. Young (1998), Identification of improved rainfall-runoff models for an ephemeral low-yielding Australian catchment, *Environ. Modell. Softw.*, *13*(1), 59–74.
Yhidego, Y., and J. A. Webb (2011), Modeling of bore hydrographs to determine the impacts of climate and land-use change in a temperate subhumid region of southeastern Australia, *Hydrogeol. J.*, *19*(4), 877–887.